Atomization Characteristics of a Double Impinging F-O-O-F Type Injector with Four Streams for Liquid Rockets

Shin-Jae Kang*, Byung-Joon Rho
Department of Mechanical Engineering, Chonbuk National University, Automobile High Technology Research Institute
Je-Ha Oh, Ki-Chul Kwon
Chonbuk Automobile Part and Mold TIC, Chonbuk National University

This paper presents atomization characteristics of a double impinging F-O-O-F type injector with four streams. A phase Doppler particle analyzer was employed to measure the droplet-size and water was used as the inert simulant liquid instead of reactive propellant liquids. The droplet mean diameter (SMD) and size distribution were measured to investigate the effects of the momentum ratio and pressure drop variations. This experimental results can be used during the preliminary design stage of a impinging stream type injector for liquid rockets.

Key Words : Liquid Rocket Fuel Injector, Impinging Type, Phase Doppler Particle Anayzer (PDPA), Sauter Mean Diameter (SMD), Momentum Ratio

Nomenclature

ΔP	: Pressure drop [psi]
$D_{0.632}$	: Drop diameter such that 63.2% of total liquid volume is in drops of smaller diameter [μm]
MMD	: Mass median diameter [μm]
MR	: Momentum ratio
$\dot{m}$	: Mass flowrate [g/s]
r	: Mixture ratio
SMD	: Sauter mean diameter [μm]
$\overline{SMD}$	: Mean SMD [μm]

Subscripts

f	: Fuel
o	: Oxidizer

1. Introduction

To develop a liquid rocket engine, analysis should be validated with experimental data. Fluid dynamic and thermodynamic phenomena in a combustion chamber of the engine affect the performance of the propulsion system. Therefore, the combustion chamber performance should be estimated accurately to develop liquid rocket engines. The element closely related to the combustion chamber performance is the propellant injector because it affects the mixing performance, atomization, and spatial distribution of propellant.

Many types of liquid rocket fuel injectors have been developed. In this study, the impinging type injector, which makes the propellant impinge on each other and produces impinging energy, was investigated. In an early work, Elverum et al. (1959) investigated empirically the optimum mixing distributions of propellents in an impinging type liquid rocket injector. Rupe (1956) also studied a correlation between the dynamic properties of a pair of impinging streams and the uniformity of mixture ratio distribution in the resulting sprays. Calhoon et al. (1973) suggested an injector design model for predicting rocket engine performance. This model quantifies the combustion performance and chamber heat flux

* Corresponding Author,
E-mail : sjkang@jnplab.chonbuk.ac.kr
TEL : +82-652-270-2387 ; **FAX** : +82-652-270-2472
Department of Mechanical Engineering, Chonbuk National University, Automobile High Technology Research Institute, 664-14, Dukjin-dong, Dukjin-gu, Chonju, Chonbuk 561-756, Korea. (Manuscript **Received** August 23, 1999; **Revised** January 12, 2000)

as functions of injector element type, element area ratio, impingement angle, mixture ratio, momentum ratio, and physical size. Also, design equations are given for combustion performance evaluation in injectors. Brault and Lourme (1985) carried out cold flow tests for characterization of Viking rocket 'line-on-line' injectors based on the extension of a Malvern sizer. Hulka and Schneider (1993) carried out the cold flow testing of an oxidizer-swirled coaxial single element injector in the Space Transportation Main Engine (STME). In their study, increasing the oxidizer injection velocity had the greatest influence on reducing oxidizer droplet size parameters and increasing the size distribution for non-gas assisted flows. Rho et al. (1998) also investigated the droplet velocity, turbulence flow properties, mean droplet size distribution, and droplet rate in a two-phase swirling jet using a Phase Doppler Particle Analyzer (PDPA) system.

Santoro et al. (1995) studied the performance of a swirl coaxial injector with various mixing conditions. Park et al. (1994) investigated the spray characteristics of an impinging doublet injector. The atomization characteristics of scaled-down versions of a coaxial rocket injector and a quadruplet rocket injector were investigated using a PDPA by Sankar et al. (1991). Specifically, they presented the effects of the gas pressure and the injector recess size on flow variables such as the mean droplet diameter, Sauter mean diameter, number density, volume flux, and droplet velocity. Rho et al. (1995) made measurements on the atomization characteristics, and derived an expression that there would be pertinent droplet size distribution functions and an absolute correlation between the SMD and mass ratio.

Propellant is atomized and mixed by the impinging energy. The double impinging type injector with four streams sprays fuel in the outward two jets and oxidizer in the inward two jets through the orifice. Water was used in lieu of fuel and propellant.

The atomized droplet size as well as the three dimensional velocity components were measured using a phase doppler particle analyzer (PDPA).

2. Test Facilities and Experimental Arrangement

Test facilities to investigate the atomization characteristics of impinging type injectors are composed of a simulant propellant feeding system, an injector and a laser measurement system.

The propellant feeding system delivers the propellant from the propellant tank to the injector. An industrial displacement pump was employed to supply the propellant continuously to the injector at high pressure and flow rate. This pump can provide a maximum discharge flow rate

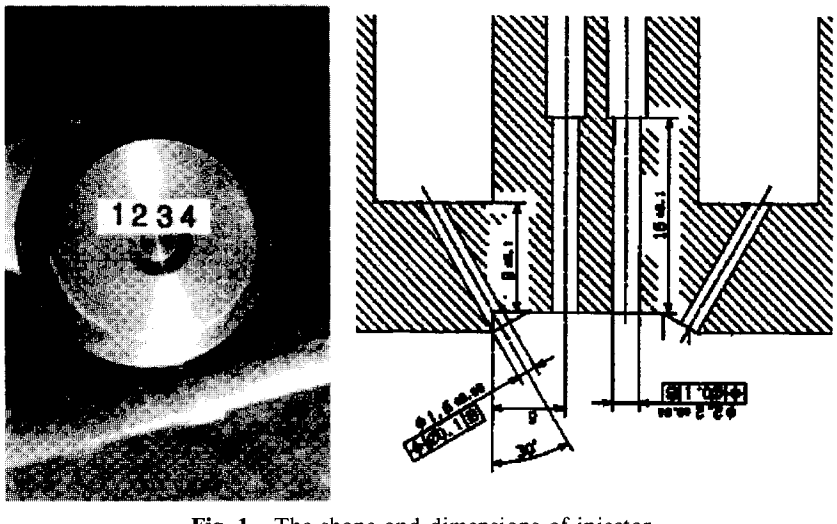

Fig. 1 The shape and dimensions of injector

Table 1 Design values of injector

Type	Double impinging type with four jet streams [F-O-O-F type]
First impinging angle (θ)	30°
First impinging length	10.39 mm
Oxidizer orifice diameter	2.2 mm
Fuel orifice diameter	1.6 mm

of 99 ℓ/min and a maximum discharge pressure of 60 kg_f/cm^2. In addition, a ball valve, which can resist high pressures, was used to control the flow rate. The supply pressure was measured just before the simulant propellant was provided to the injector.

The injector is an F-O-O-F type in which the outward two fuel jets impinge onto the inward two oxidizer jets. Thus, the propellant is mixed and atomized.

The specification of the uni-element injector applied in this study is shown in Fig. 1 and Table 1. Fuel is injected through the Orifices ① and ④ and oxidizer through the Orifices ② and ③. The fuel stream through Orifice ① initially impinges onto the oxidizer stream from ②. (③ impinges onto ④) These impinged jets impinge again and then form the impinging sprays.

The first impinging length is the distance from the center of the orifice exit plane to the point where the centers of the fuel and oxidizer streams first impinge. When the impinging length is long, it causes bad atomization because the splitting length becomes long. On the other hand, when the impinging length is short, it results in a burnout of the injector plane by the wake flow. Therefore, the first impinging length was set to be 10.39 mm in this study. An impinging angle is closely related to the wake flow of propellant, The uniformity of mixture, the atomizing length of the spray, the atomized droplet size, and the width of the spray. When the impinging angle is small, mixture becomes better but the impinging length becomes long. When the impinging angle is large, atomized droplet size becomes small but the wake

Table 2 Spray conditions

(Unit $\dot{m}$: g/s, P : kPa)

(a)

r	MR	$\dot{m}_f$	$\dot{m}_o$	P_f	P_o
1.50	1.19	104.0	156.0	725.3	532.5
2.00	2.12	86.70	173.3	503.5	657.7
2.47	3.22	75.00	185.0	377.1	749.5
3.00	4.76	65.00	195.0	283.2	832.2
3.50	6.48	57.80	202.2	223.8	895.0

(b)

r	MR	$\dot{m}_f$	$\dot{m}_o$	P_f	P_o
1.24	0.81	101.4	125.5	689.5	344.7
1.52	1.21	101.4	153.7	689.5	517.1
1.75	1.62	101.4	177.5	689.5	689.5
1.96	2.02	101.4	198.4	689.5	861.8
2.47	3.24	71.71	177.5	344.7	689.5
2.02	2.16	87.83	177.5	517.1	689.5
1.75	1.62	101.4	177.5	689.5	689.5
1.57	1.30	113.4	177.5	861.8	689.5

flow of mixed propellant increases and causes the burnout of the injector plane. As a result, the impinging angle was determined within a range applied ordinally in the impinging injector.

Three dimensional phase doppler particle analyzer (PDPA) was employed to measure the atomized droplet size and velocity components.

PDPA consists of an optical system, a signal processing system and a three dimensional traversing system. The optical system is composed of transmitting & receiving optics, and a 350mW air-cooled Ar-ion laser was used. Transmitting optics make three different laser beams cross at the measurement point. Receiving optics detect the scattered light, which is produced when droplets pass through the measurement volume, and then transmit it to the signal processor. The signal processor (DANTEC model 58N50) is a burst detector type. Therefore, the size and velocity are measured by the frequency and relative phase difference of the Doppler signal.

The voltage provided to the receiving optic

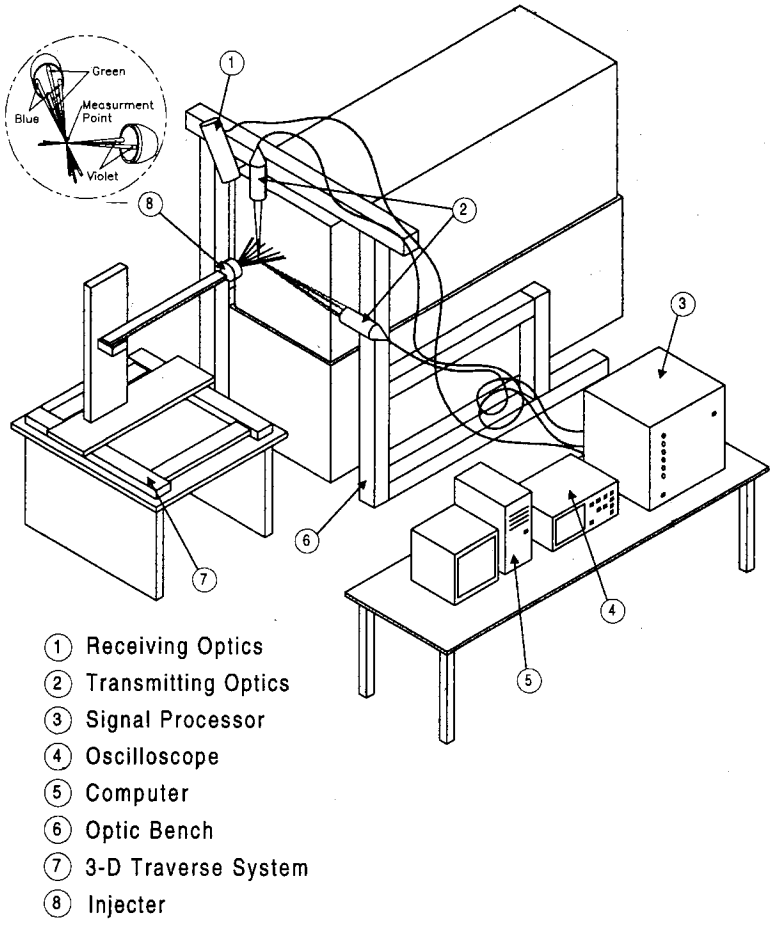

Fig. 2 Schematic diagram of PDPA System

sensor was fixed at 1400 V. At each measurement point, 10,000 droplets were sampled and sampling time was limited to within 10 seconds.

Water was used instead of propellant liquids. Atomized droplet size was measured for various oxidizer/fuel ratios. The total flow rate was fixed at 260 g/s. A change of momentum ratio means a change in the mixture ratio ($r=\dot{m}_o/\dot{m}_f$). Moreover, the droplet size was measured by changing the pressure drop of fuel or oxidizer. When the pressure drop of fuel is changed, the pressure drop of oxidizer is fixed. When the pressure drop of oxidizer is changed, the pressure drop of fuel is fixed. Table 2 shows the experimental conditions.

When the momentum ratio was changed (Table 2(a)), the droplet size was measured at the axial distance of 20 mm, 30 mm, 50 mm and 100 mm. Each cross section has 21×21 measurement points. When the pressure drop was changed (Table 2(b)), the droplet size was measured at 50 mm and 100 mm.

3. Results and Discussion

The impinging injector used in this study has a considerable droplet size compared with other types of injectors because it has a large orifice diameter and a high flow rate unlike the others such as pressure atomizer.

The droplet size distributions are depicted in Fig. 3 for the momentum ratio of fuel and oxidizer under the fixed total flow rate at 260 g/s. As seen from the cross section at x=20 mm, 30 mm and 50 mm in Fig. 3, there is an unmeasured area

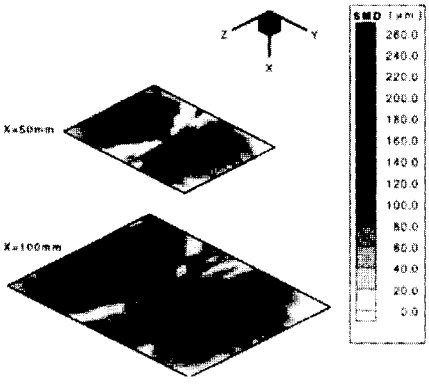

(a) r=1.50, MR=1.19

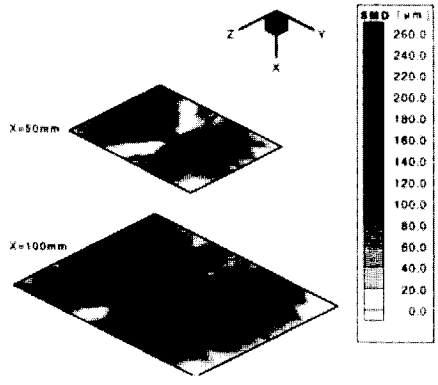

(b) r=2.00, MR=2.12

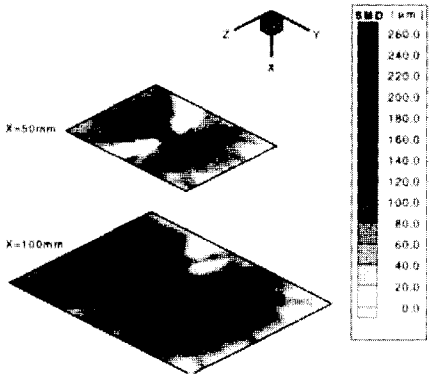

(c) r=2.47, MR=3.22

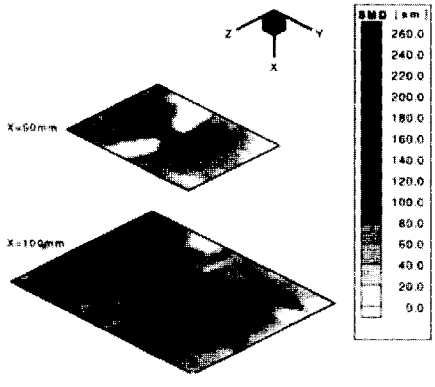

(d) r=3.00, MR=4.76

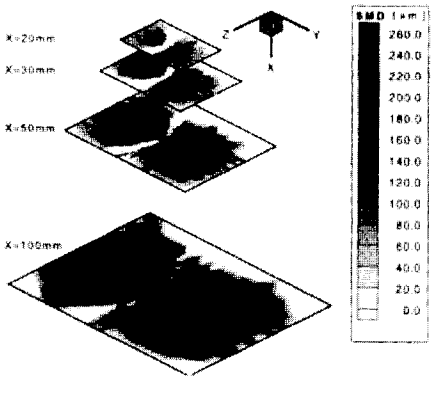

(e) r=3.50, MR=6.48

Fig. 3 Iso-drop size(SMD) contours with momentum ratio

near the center of the spray. It is assumed that the causes would be the effects of high mass flux of the spray flow field and impinging jets in a liquid sheet condition unsplitted to droplets. Figure 3 shows that the SMD of droplets increases as the distance of axial locations becomes long. The SMD of droplets increases for momentum ratios between 1.19 and 2.12. However, it declines for

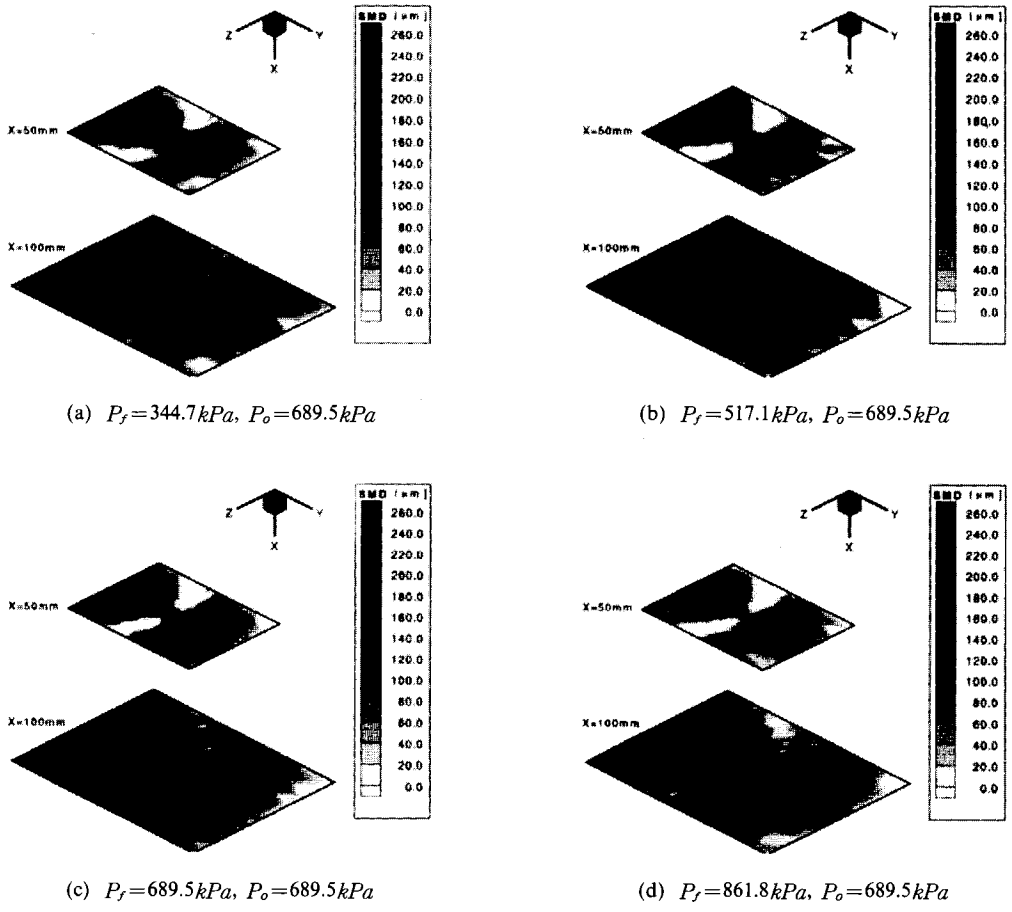

(a) $P_f=344.7kPa$, $P_o=689.5kPa$ (b) $P_f=517.1kPa$, $P_o=689.5kPa$

(c) $P_f=689.5kPa$, $P_o=689.5kPa$ (d) $P_f=861.8kPa$, $P_o=689.5kPa$

Fig. 4 Iso-droplet size(SMD) contours with fuel pressure drop

momentum ratios between 2.12 and 6.48. The former result occurs because the momentum decrease of outer fuel jets have an influence on the spilt of droplets greater than the momentum increase of inner oxidizer jets. The latter result is due to the momentum increase of inner jets. However, the SMD becomes larger near the center of the spray as the momentum ratio increases. The reason for this is that the split of droplets is processing in the center of the spray because the splitting length increases on account of the effect of the momentum increase of inner jets.

Figure 6 shows the mean values of SMD at every point for x=50 mm and 100 mm away from the injector plane. While the $\overline{SMD}$ at x=50 mm generally increases as the momentum ratio goes up, the $\overline{SMD}$ at x=100 mm decreases. The maximum $\overline{SMD}$ occurs at x=100 mm, when the momentum ratio is 2.12. These results are similar to Kang's result (1999) in which the SMD of droplets was measured for various momentum ratios of oxidizer and fuel under the fixed total flow rate. According to Kang (1999), the $\overline{SMD}$ of droplets increases for momentum ratios between 0.64 and 1.78, but it decreases for momentum ratios above 1.78. The results from this study suggest that the $\overline{SMD}$ increases for momentum ratios between 1.78 and 2.12, and that it declines for momentum ratios above 2.12. Therefore, when momentum ratios are changed under the fixed total flow rate, these trends are satisfied. However, the momentum ratio should be neither high nor low. When the momentum of inner streams is low, it is likely to affect the spray flow field badly because of the wake flow. The latter occurs because the inner jets do not go

completely to the axial location after impinging onto the outer jets at the exit plane. When the momentum of inner streams is high, the spray form will likely be similar to the pressure atomizer and atomization will likely be dependant on the pressure drop variation of the inner jets. This is because the outer jets cannot break through the inner jets. Thus, only two inner jets proceed.

Moreover, the $\Delta\overline{SMD}$ ($\overline{SMD}_{x=100mm} - \overline{SMD}_{x=50mm}$) declines as the momentum ratio increases (Fig. 6). This is because the momentum increase of inner streams results in the small reduction of inertia force as droplets move to the axial direction.

Figure 4 presents the SMD distribution of the impinging spray flow field with increasing the pressure drop variation of outer fuel streams from 344.7 kPa to 861.8 kPa at intervals of 172.4 kPa under the fixed pressure drop(ΔP) of inner oxidizer streams at 689.5 kPa. Figure 5 presents the SMD distribution with increasing pressure drop variation of inner oxidizer streams from 344.7 kPa to 861.8 kPa at intervals of 172.4 kPa under the fixed pressure drop of outer fuel streams at 689.5 kPa.

As shown in Fig. 4, when the pressure drop of outer streams increases, the SMD at the central point and other points decline. This tendency coincides with the results of Park (1996). $\overline{SMD}$ decreases with increasing pressure drop at x=50 mm and 100 mm as shown in Fig. 6. When the pressure drop of inner jets is fixed, the pressure drop variation of outer jets is the significant factor which affects atomization of the spray flow field. In addition, the $\Delta\overline{SMD}$ between x=50 mm and x=100 mm increases because the relative increase of impinging momentum expedites atomization in the front end of the spray flow field.

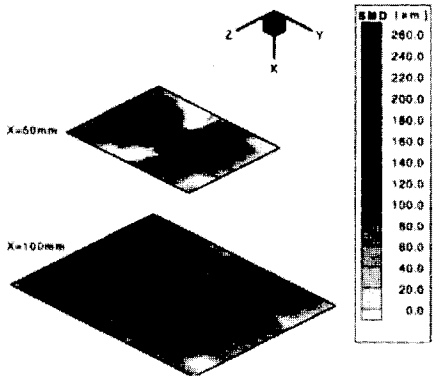

(a) P_f=689.5kPa, P_o=344.7kPa

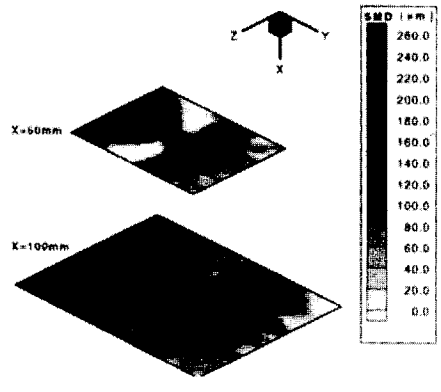

(b) P_f=689.5kPa, P_o=517.1kPa

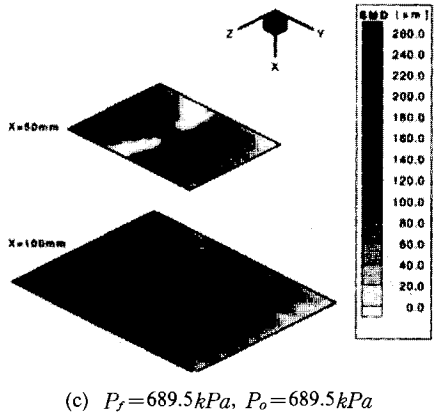

(c) P_f=689.5kPa, P_o=689.5kPa

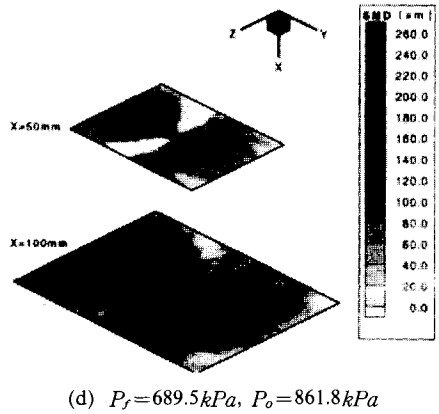

(d) P_f=689.5kPa, P_o=861.8kPa

Fig. 5 Iso-droplet size(SMD) contours with oxidization pressure drop

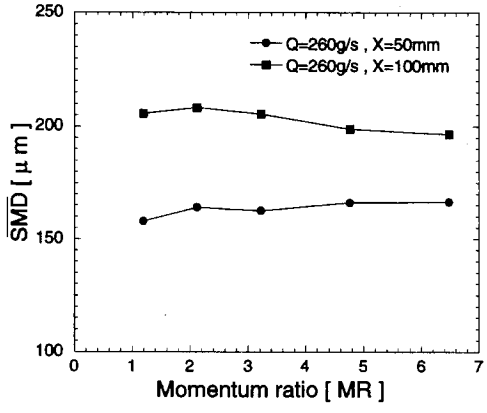

(a) $\dot{m}_f+\dot{m}_o=260$g/s

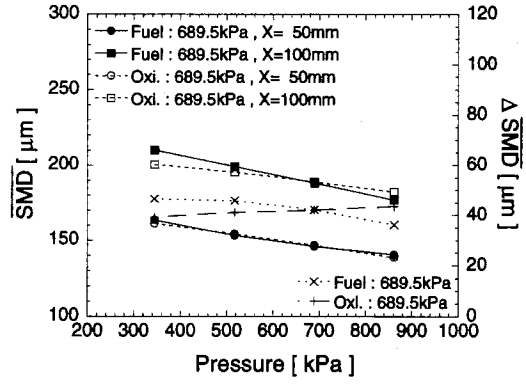

(b) $\Delta P=100psi$

Fig. 6 Variation in mean droplet size($\overline{SMD}$) with momentum ratio and pressure drop

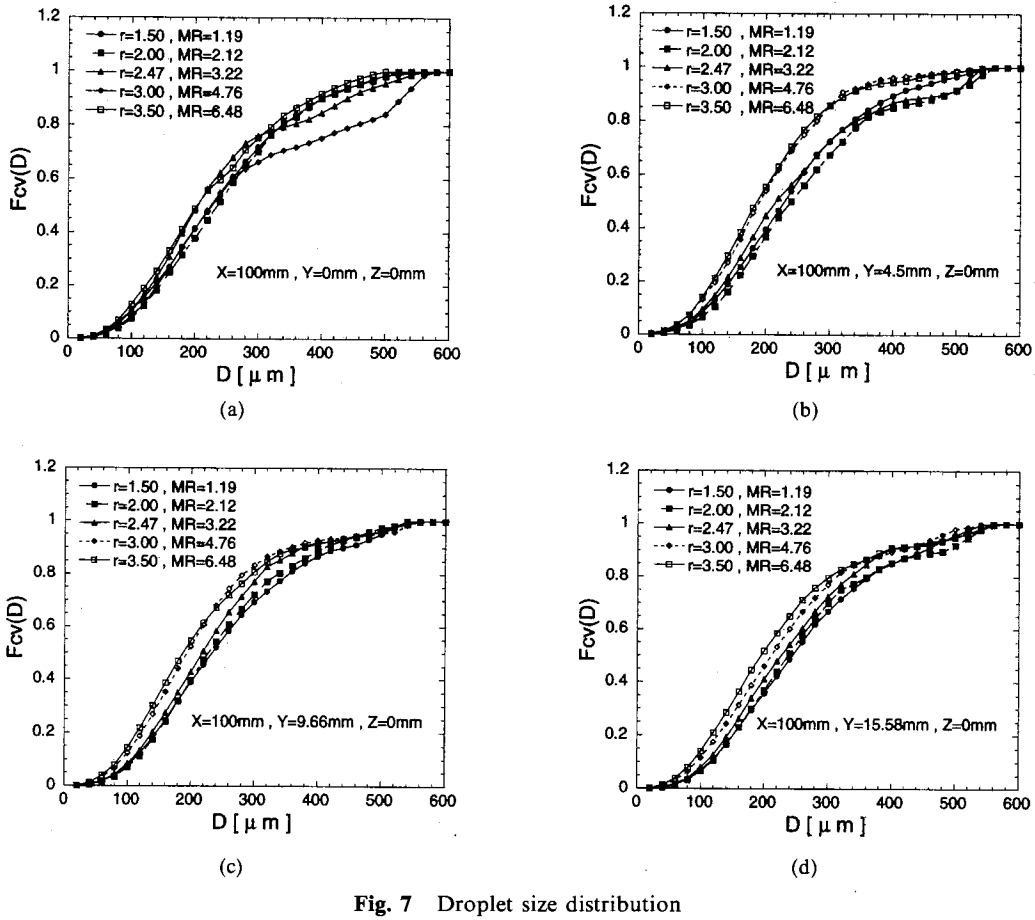

Fig. 7 Droplet size distribution

However the relative decrease of droplet inertia force is higher than that of the impinging momentum after front end.

Figure 5 shows the SMD distribution vs the pressure drop variation of inner oxidizer streams under the fixed pressure drop of outer fuel streams at 689.5 kPa. The SMD declines as the pressure drop of inner oxidizer increases. However, the

SMD in the center of the spray is similar, as shown in Fig. 5. In Fig. 6, the $\overline{SMD}$ and the $\Delta\overline{SMD}$ between x=50 mm and x=100 mm decrease as the pressure drop increases because the relative decrease of inertia force is lower than that of the impinging momentum for increasing pressure drop of inner jets. This result is different from the study of Park (1996). It is possible that the following factors cause this difference. The injector used in the study of Park (1996) is the triplet O-F-O type. The fixed pressure drop ratio and the supply flow rate are different in this study. Park (1996) measured the SMD at the central point at x=75 mm, but, in this study, the SMD was measured at all points in the cross sections perpendicular to the spray flow field.

Graphics of the cumulative volume distribution vs momentum is shown in Fig. 7. The Rosin-Rammler distribution function (Rosin and Rammler, 1939) and the Upper-limit distribution function (Mugele and Evans, 1951), which are used frequently to express a droplet size distribution mathematically, are obtained from the measured droplet size distributions. The measured droplet size distribution is compared with the Rosin-Rammler distribution function and the Upper-limit distribution function in Fig. 8.

As shown in Fig. 7, $D_{0.632}$, X, and $D_{0.5}$ which presents mass median diameter (MMD) increase as the momentum ratio increase. The cumulative volume taken up by small droplets also increases as the momentum ratio increases, but it is the least when the momentum ratio is 2.12.

$$1-Q=\exp-\left(\frac{\ln D}{\ln X}\right)^q \tag{1}$$

In Fig. 8, the cumulative volume distributions of measured droplets are compared with the Rosin-Rammler distribution function and the Upper-limit distribution function. The Number distribution is also compared with the Log-normal distribution function. According to Fig. 8, the cumulative volume distribution of measured droplets match with the Rosin-Rammler distribu-

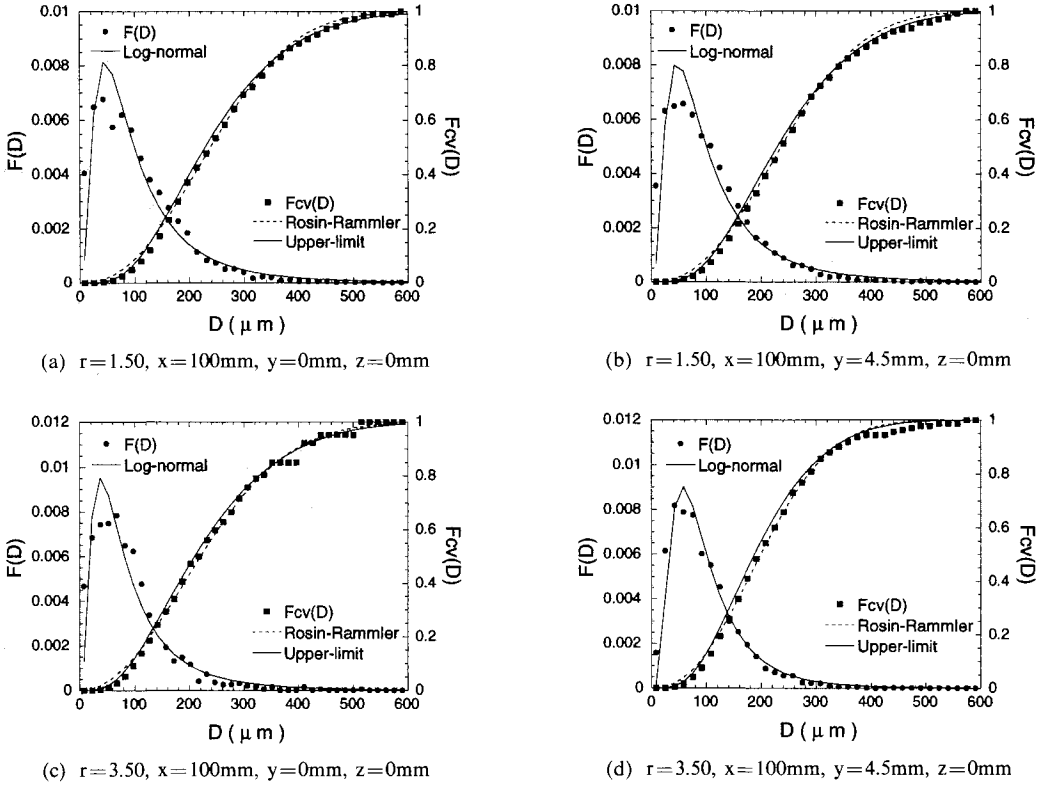

(a) r=1.50, x=100mm, y=0mm, z=0mm

(b) r=1.50, x=100mm, y=4.5mm, z=0mm

(c) r=3.50, x=100mm, y=0mm, z=0mm

(d) r=3.50, x=100mm, y=4.5mm, z=0mm

Fig. 8 Droplet size distribution function

tion function and the Upper-limit distribution function. The Number distribution and the Log-normal distribution function also match.

However, when the droplet size section is divided into small, medium and large parts, the Upper-limit distribution function coincides well in the small and large parts. However, it inclines to the left in the medium part where MMD and $D_{0.632}$ are included. On the other hand, the Rosin-Rammler distribution function does not match in the small and large parts, but it does well in the medium part. The Upper-limit distribution function coincides well in the small and large parts because it finds the appropriate value using a trial-and-error method which assumes the maximum and the minimum value of droplets. The Rosin-Rammler distribution function matches well in MMD and $D_{0.632}$ because $D_{0.632}$ is the significant variable in the Rosin-Rammler distribution function.

For the Log-normal distribution function and the Number distribution which presents the density of probability of measured droplet size, the droplets which have the maximum density of probability comparatively coincide. However, the maximum density of probability calculated by the Log-normal distribution function is higher than the measured maximum density of probability.

4. Conclusions

The study investigated the atomization characteristics versus pressure drop and momentum ratio variation in a double impinging F-O-O-F type injector. The results are as follows.

The SMD of droplets is decreased as the momentum ratio of fuel and oxidizer increases under the fixed total flow rate. In addition, the SMD distribution at MR=2.12(r=2.00) is the largest. The difference between $\overline{SMD}$ at x=50 mm and x=100 mm declines as the momentum ratio increases. The SMD and $\overline{SMD}$ in the cross sections for the momentum ratio variation are similar. It is believed that the mean value of all SMD at every point in the cross sections, $\overline{SMD}$, is better for investigation of atomization characteristics than the SMD at one point.

Both $\overline{SMD}$ at x=50 mm and 100 mm as well as the difference between the two decrease as the pressure drop of oxidizer increases under the fixed pressure drop of fuel at 689.5 kPa. Both $\overline{SMD}$ at x=50 mm and 100 mm decrease as the pressure drop of fuel increases under the fixed pressure drop of oxidizer at 689.5 kPa, but the difference between the two increases somewhat.

Droplet size distributions measured in the impinging spray flow field coincide well with the Upper-limit distribution function in small and large parts. Droplet size distributions match with the Rosin-Rammler distribution function in the medium part where MMD and $D_{0.632}$ are included. Droplet size of MMD and that of $D_{0.632}$ decline as the momentum ratio increases.

References

Brault, F. and Lourme, D., 1985, "Experimental Characterization of the Spray Formed by Two Impinging Jets in Liquid Rocket Injector," ONERA TP No. 1985-68.

Calhoon, D. F., Kors, D. L. and Gordon. L. H., 1973, "An Injector Design Model for Predicting Rocket Engine Performance and Heat Transfer," AIAA Paper 73-1242.

Elverum, G. W. and Morey, T. , 1959, "Criteria for Optimum Mixture Ratio Distribution Using Several Types of Impinging Stream Injector Elements," Memorandum 30-5, Jet Propulsion Lab. Calif. Inst. Tech.

Hulka, J. and Schneider, J. A., 1993, "Single Element Injector Cold Flow Testing for STME Swirl Coaxial Injector Element Design," *AIAA, SAE, ASME, and ASEE, Joint Propulsion Conference and Exhibit, 29th*, Monterey, CA.

Huzel, D. K. and Huang, 1992, Modern Engineering for Design of Liquid-Propellent Rocket Engines, AIAA, Washington, pp. 104 ~115.

Kang, S. J., Oh, J. H., Park, S. M., Kwon, K. C., and Che, Y. S., 1999, "An Experimental Study on Spray Characteristics of Impinging Type Injector for Liquid Rocket," *Proceeding of the KSAS 1999 Spring Annual Meeting*, pp. 314 ~317.

Lefebvre, A. H., 1989, *Atomization and Spray*, Hemisphere Publishing Co., pp. 79~103.

Mugele, R. and Evans, H. D., 1951, "Droplet Size Distribution in Sprays," *Ind. Eng. Chem.*, Vol. 43, No. 5, pp. 1317~1324.

Park, S. Y., Kim, S. J., Park, S. W. and Kim, Y., 1996, "A Study on Spray Characteristics of the Triplet Impinging Stream Type Injector for Liquid Rocket," *Transactions of KSME*, Vol. 20, No. 3, pp. 1005~1014.

Rho, B. J., Kang, S. J., and Oh, J. H., 1995, "An Experimental Study on the Atomization Characteristics of a Two-Phase Turbulent Jet of Liquid Sheet Type Co-Axial Nozzle," *Transactions of KSME*, Vol. 19, No. 6, pp. 1529~1538.

Rho, B. J., Kang, S. J., Oh, J. H., and Lee, S. G., 1998, "Swirl Effect on the Spray Characteristics of a Twin-Fluid Jet," *KSME International Journal*, Vol. 12, No. 5, pp. 899~906.

Rosin, P. and Rammler, E., 1939, "The Laws Governing the Finess of Powered Coal," *J. Inst. Fuel*, Vol. 7, No. 31, pp. 29~36.

Rupe, J. H., 1956 "A Correlation Between the Dynamic Properties of a Pair of Impinging Streams and the Uniformity of Mixture Ratio Distribution in the Resulting Spray," Prog. Rep. 20-209, Jet Propulsion Lab. Calif. Inst. Tech.

Sankar, S. V., Brenadelarosa, A., Isakovic, A., and Bachalo, W. D., 1991, "Experimental Investigation of Rocket Injector Atomization," *The 28th JANNAF Combustion Subcommittee Meeting*, Vol. 2, pp. 187~198.

Santoro, R. J., Pal S., and Rahman, 1995, "Swirl Coaxial Atomization; Cold-Flow and Hot-Fire Experiments," AIAA 95-0381

Sutton, G. P. and Ross, D. M., 1976, *Rocket Propulsion Elements*, John Wiley & Sons, Inc., USA, pp. 286~295.